PERIODICA POLYTECHNICA SER. MECH. ENG. VOL. 50, NO. 1, PP. 57–66 (2006)

EXPERIMENTAL STUDY OF THE FRICTION TORQUE ON A DISC ROTATING IN VISCOUS FLUID AROUND ITS HORIZONTAL DIAMETER

Csaba TIZEDES and Csaba HŐS

Department of Hydrodynamic Systems
Faculty of Mechanical Engineering
Budapest University of Technology and Economics
H–1521 Budapest, Hungary
e-mail: hoscsaba@vizgep.bme.hu

Received: April 10, 2006

Abstract

If a disc is rotated in a fluid around its diameter, a reaction torque arises due to the viscosity of the fluid. In this study, we present the results of an experimental analysis of such a motion. Discs of several diameter have been rotated in water, while the torque and revolutionary speed has been recorded. The data sets are interpreted with the help of dimensionless quantities. Based on the experimental data, analytical formulae are given for the torque-angular velocity relationship and for the critical Reynolds number at which the laminar-turbulent transition occurs.

Keywords: fluid damping torque, rotating disc, Euler number, curve fitting.

Nomenclature

A	[m^2]	cross-section
D, d	[m]	diameter (disc, crabs)
E	[GPa]	elasticity modulus
F	[N]	force
g	[m/s^2]	gravitational acceleration
h	[m]	thickness
m	[kg]	mass
M	[Nm]	friction torque
n	[rpm]	revolution number
p	[ ]	relative deviation
x	[...]	abscissa of measured point
y	[...]	ordinate of measured point

Eu	[ ]	Euler number
Fr	[ ]	Froude number
Re	[ ]	Reynolds number
rho	$[kg/m^3]$	density
nu	$[m^2/s]$	kinematic viscosity
ω	$[rad/s]$	angular velocity
σ	$[GPa]$	stress, except par.3
σ	[...]	standard deviation, only in par.3
ε	[-]	strain

Subscripts

$cable$	cable
$crit$	critical
d	disc
f	fluid

1. Introduction

When analysing the motion of rigid bodies moving in fluids, the Newtonian equations of motion include the damping torque of the fluid due to the fluid viscosity. One of the most common application is the calculation of power requirement of mixing apparatus (for general description, see [1]). Similarly, if the motion forms of a slender body falling freely in viscous fluid (e.g. motion of falling autumn leaves) is to be computed, this torque plays a decisive role in deciding whether rocking motion (pendulum-like motion), autorotation (continuous rotation) or chaotic motion appears (an example of such analysis is given in [4]). A third example is the dynamic analysis of hydraulic check valves, which is (roughly speaking) an eccentric disc with weight load mounted into a pipe, which allows flow only in one direction and is used typically at the pressure side of pumps for preventing back-flow (for details, see [5]).

This paper is motivated by an industrial application. The task was to compute the number of collisions of a maverick circular metal cover inside a vertical pipe in which fluid flows upwards. The number of collisions was needed in order to give an estimation for calculating fatigue load. The estimation was given by integrating the equations of motion (for the cover) with appropriate event handling algorithm and impact law for locating the collisions and for restarting the integration, respectively. However, it was found that little is known about the dependence of the fluid breaking torque on the angular velocity, slenderness or other parameters (e.g. the geometry of the surrounding space) if the body is a disc rotating around its diameter. This is mainly due to the fact that in the case of mixing apparatus, this body shape is hardly used, see [1]. However, for regular mixing paddles, an enormous number of measured values is available - for pairs of mixer elements and tanks. From the

practical point of view, the Euler number (dimensionless breaking torque or loss coefficient) is important as a function of the Reynolds number (which is – roughly speaking – a dimensionless angular velocity). A common feature of all mixing elements is that for small Re numbers (typically below 10 60) the flow is laminar and Eu Re^{1} while for large Re numbers (typically above 10^3 10^4), the flow is turbulent and the Euler number is constant. The $Eu(Re)$ relationship in the transition region is usually determined by measurements.

The aims of the experimental work presented in this paper are *(i)* to give a closed-form estimation of the $Eu(Re)$ relationship for thin circular discs (possibly using dimensionless quantities), *(ii)* to give an estimation for the critical Reynolds number corresponding to the laminar-turbulent transition and, *(iii)* to study the effect of the disc thickness.

2. Experimental setup

The basic principle of the measurement can be summarized as follows. Referring to *Fig. 1* and *Fig. 2*, the disc (1) is mounted onto a shaft (8) with bearings (7) and adequate support (2). At the end of the shaft, a crab (3) with thin cable (fishing-line) (4) is located, through which the disc can be rotated. The whole apparatus is submerged into water. The cable is then led through a divided disc (5) for the measurement of the revolutionary speed, which is located high above the water level. Different weights (6) are hung at the end of the cable. As these weights sink vertically, the disc – after a short accelerating period – rotates with a constant angular velocity. If the inner frictions (e.g. in the bearings) can be neglected, the damping torque of the fluid is simply the torque exerted by the weights. Friction losses are estimated by the fact that the shaft – in the air without disc – started to rotate if the weight exceeded 0.05 kg. The diameter of the crab on the disc shaft was 31 mm and the other one on the divided disc was 45 mm. The width of the water channel into which the apparatus was submerged was 0.7 m and the depth of the water was minimum 1 m.

To record the angular velocity, a divided disc (5) with an optical sensor was used. The width of the devision was 10 degrees and as the disc rotates, the devisions cut the signal of the photodiode. The signal is then led to a Schmitt trigger, which converts the analogue signal of the photocell into a digital one. This digital signal is then recorded by a HBM Spider 8 data acquisition equipment. The rough data sets are then processed with Matlab to give the angular velocity ω and final results are obtained with Excel. Every measurement (i.e. fixed disc diameter and weight) was performed at least three times. Typical $M_f(\omega)$ graphs are plotted in *Fig. 3*. Note that the scale on both axis is logarithmic to highlight the fact that for small angular velocities, the slope is approx. 1 and hence the flow is laminar, while for larger values of ω, the slope increases.

Let us turn now to the accuracy of the measurements. We only give here the error bounds without going into details. Should the reader have a deeper

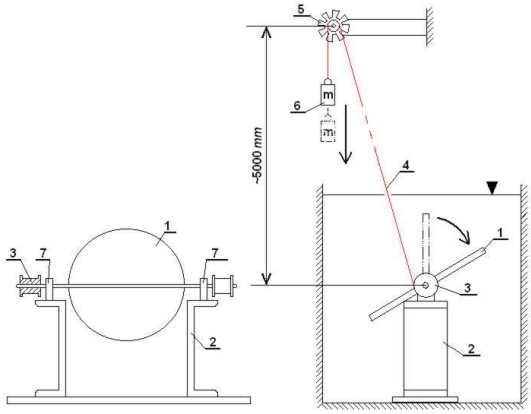

Fig. 1. The shafted disc with the support (for details, see the text).

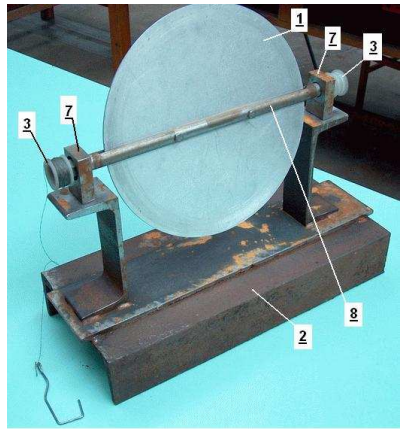

Fig. 2. The experimental setup.

interest of the estimation, the authors are happy to provide further information. Density and viscosity are considered to be temperature-dependent. At constant temperature, the error in density and viscosity of the water due to the accuracy of the temperature measurement (0.1^oC) was ρ (998.22 0.02) kg/m^3 and ν (1.004 0.0025) mm$^2/s$. The relative error of the diameter due to manufacturing was below 0.02% for each disc. The relative angular error of the devisions on the divided disc was below 1.7%. By using elementary geometry, it can be shown that assuming 1 mm assembling eccentricity of the divided disc, the relative angular error is below 1.5% (compared to the theoretical value of 10 degrees). No slip was observed between the divided disc and the cable.

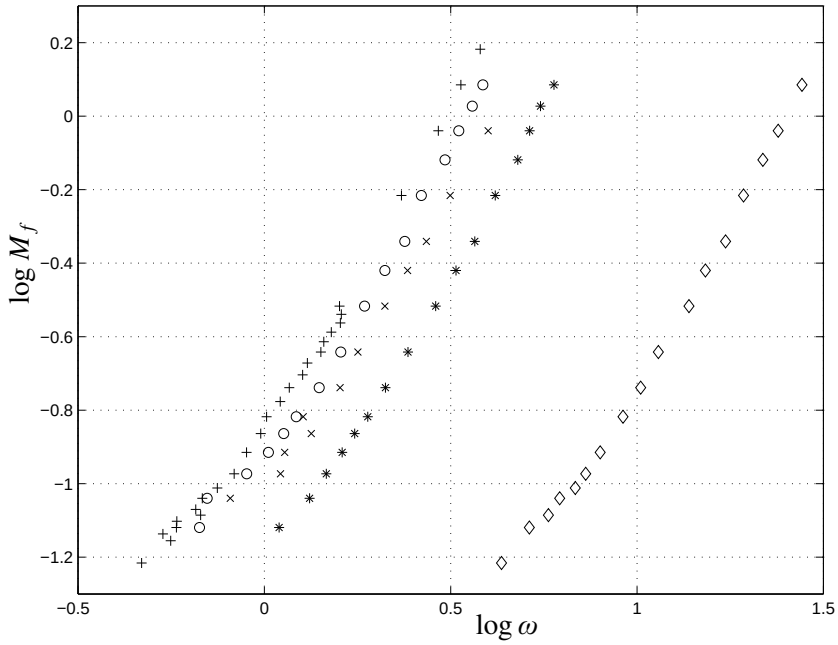

Fig. 3. Braking torque of the fluid as a function of the angular velocity, experimental results for D=120mm (diamond), D=224mm (asterisk), D=251mm (cross), D=270mm (circle) and D=285mm (plus sign).

It should be also studied whether the elastic expansion of the cable causes a considerable error. The material of the cable is assumed to be linearly elastic, i.e. the Hooke law holds and we have $\sigma \quad \varepsilon E$, where σ denotes the stress and ε stands for relative lengthening, $\varepsilon \quad \Delta L/L$. E is the elasticity modulus of the cable, which was found to be $E \quad 59.6$ GPa. If the diameter of the crab on the disc underneath the water is denoted by d_3 and that one of the divided disc is d_5 (see *Fig. 1*), then for the ideal (non-elastic) case, we have $d_3\,\omega_3 \quad d_5\,\omega_5$. However, if the cable stretches between the two discs, we have

$$\omega_5 \quad \left(1 \quad \frac{m\,g}{A_{cable}\,E}\right)\frac{d_3}{d_5}\omega_3 \quad \left(1 \quad \frac{m\,kg}{298\,kg}\right)\frac{d_3}{d_5}\,\omega_3, \tag{1}$$

where m is the mass of the weight, g is the gravitational acceleration and A_{cable} is the cross-sectional area of the cable. The second part of the above equation (1) gives the real, measured angular velocity. Taking into account that the largest weight applied during the measurements was 4 kg, we see that the relative error is below 1.3%.

However, by calculating the *empirical* standard deviation of the angular de-

viation, we experienced a relative deviation up to 8% in terms of angular velocity. We speculate that this large error is due to the recording of the velocity and the computer data processing. Finally, the empirical relative standard deviation of the torque was below 0.16%.

3. Dimensionless Parameters

In this section, we introduce dimensionless quantities, which allow us to reduce the number of parameters describing the phenomena under investigation.

We have eight parameters describing the experiments, i.e. disc diameter D m, disc thickness h [m], disc and fluid density ρ_d [kg/m^3] and ρ_f [kg/m^3], kinematic viscosity of the fluid ν [m^2/s], gravitational acceleration g [m/s^2], disc revolutionary speed n [rpm] and braking torque M_f [Nm]. Applying dimension analysis (for details, see [3]), the following 5 dimensionless groups are derived:

$$\Pi_1 \quad \frac{h}{D} \quad \text{slenderness or relative disc thickness,} \tag{2}$$

$$\Pi_2 \quad \frac{\rho_d}{\rho_f} \quad \text{relative density,} \tag{3}$$

$$\Pi_3 \quad \frac{D^2 n}{\nu_f} \overset{def.}{=} Re \quad \text{Reynolds number,} \tag{4}$$

$$\Pi_4 \quad \frac{D n^2}{g} \overset{def.}{=} Fr \quad \text{Froude number and} \tag{5}$$

$$\Pi_5 \quad \frac{M_f}{D^5 \rho_f n^2} \overset{def.}{=} Eu \quad \text{Euler number.} \tag{6}$$

Our primary aim was to describe the $M_f(\omega)$ relationship, whose dimensionless equivalent is the $Eu(Re)$ relationship. The slenderness parameter Π_1 is a free parameter, thus we have $Eu(Re, \frac{h}{D})$. The density ratio is ignored in what follows as the authors did not study other fluid-disc pairs than water and aluminium. The only parameter left is the Froude number, which, in the case of mixing elements, describes the importance of whirl formation. However, in our case – due to the geometrical configuration – no whirl formation is expected as the gravitational and the centrifugal forces are parallel. The Froude number in our case was used to qualify the measurements as follows. By virtue of the above equations, we have

$$Fr \quad \frac{\nu_f^2}{g} \frac{1}{h^3} \left(\frac{h}{D}\right)^3 Re^2 \overset{def.}{=} A \, \Pi_1^{\alpha} \, Re^{\beta}. \tag{7}$$

Note that the parameter A was constant during our measurements (for constant temperature). It is clearly seen from (7) that α 3 and β 2 and A can be also directly computed. However, by using 'blindly' least-square technique to compute

α, β and A from the measured data and then comparing them to the theoretical values gives us valuable information about the accuracy of our measurements. *Table 1* compares the actual values obtained from the experimental results and the theoretical values. We experience a reasonable agreement between the measured and theoretical values of α and β and a significant disagreement in the case of A. It can be shown that the error of the disc thickness dominates (the corresponding standard prescribes 0.12 mm, which is 6% relative error (compared to disc thickness h=2 mm). We emphasize again that (7) does not have a theoretical significance but provides information about the accuracy of the measurement.

Table 1. Comparison of the experimental and theoretical values of A, α and β in (7).

	A	10^6	α	β
Measurements	13.7	2.6	2.93	1.998
Theory	10.08		3	2

It would be advantageous if while varying the Reynolds number (the angular velocity), only the Euler number (the braking torque) would change. Of course, the Froude number also changes when the angular velocity varies. However, one can define two new dimensionless parameters as

$$\Pi_{34} \quad \frac{Re^2}{Fr} \quad \frac{D^3 g}{\nu_f^2} \quad \text{and} \quad \Pi_{45} \quad Fr^5\, Eu \quad \frac{n^8 M_f}{g^5 \rho_f}. \tag{8}$$

Note that Π_{34} is independent of n and Π_{45} does not include D. (Π_{34} is often called Galilei number, see [1].) For the measurements, five discs were used with a diameter series that gives a linear distribution for Π_{34} between the minimal and maximal diameter values. The diameter series is D 120, 224, 251, 270 and 285 mm.

The uncertainty of the Re and Eu number can be computed in the standard way as follows. Suppose that the physical quantity y is an algebraic function of several measured variables x_i, with exponents a_i, i.e. y $K \prod_i x_i^{a_i}$, with some constant K. The standard deviation of every x_i is denoted by σ_{x_i}. The relative deviation of y is then

$$\left(\frac{\sigma_y}{y}\right)^2 \quad \sum_i \left(a_i \frac{\sigma_{x_i}}{x_i}\right)^2. \tag{9}$$

After performing the actual calculations, one obtains p_{Re} σ_{Re}/Re 8.2% and p_{Eu} σ_{Eu}/Eu 16.4%. Note that the main error source is the data acquisition technique used for measuring the angular velocity.

4. Results

The assumed form of the $Eu(Re)$ relationship is

$$Eu \quad f(Re) \quad Eu_{\text{turb}} \sqrt{1 \quad \frac{Re_{\text{crit}}^2}{Re^2}}, \tag{10}$$

where the unknown parameters Eu_{turb} and Re_{crit} are yet to be defined. It should be emphasized here that the above formula is independent of the physics, however, its advantages are (a) for small Reynolds numbers (10) it is a linear function with 1 slope, (b) for large Re numbers, it provides a constant Eu number and (c) the parameters Eu_{turb} and Re_{crit} have physical meaning as for small and large Re numbers, we have

$$\text{for} \quad Re \quad 0 \qquad \log Eu \quad \log Eu_{\text{turb}} \quad \log Re_{\text{crit}} \quad \log Re \quad \text{and} \tag{11}$$

$$\text{for} \quad Re \qquad \log Eu \quad \log Eu_{\text{turb}}. \tag{12}$$

The coordinates of the intersection of the above two linear functions is (Re_{crit}, Eu_{turb}). The unknown parameters Re_{crit} and Eu_{turb} can be determined by minimizing the RMS value of the errors as follows.

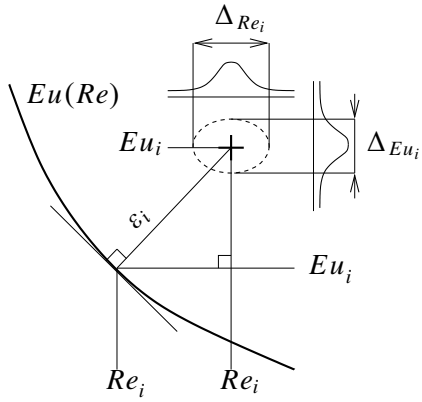

Fig. 4. Curve fitting to data points, see equation (13).

First of all note that both the Re_i co-ordinates and the Eu_i co-ordinates are known with approximately the same relative error bound. Thus, least square technique cannot be employed. Wald's method (see [2] or [6]) could overcome this difficulty but the distribution of our measurement points is not suitable for this technique, as most data points lie in the middle of the measured interval (also this technique is developed for linear functions). The parameters in (10) were determined in the following way.

Let p_{Re} and p_{Eu} denote the relative deviation of the Reynolds and Euler numbers respectively. Note that these are constants over the data set. The error bounds around the data points Re_i and Eu_i are Δ_{Re_i} 2 1.96 p_{Re} Re_i and similarly Δ_{Eu_i} 2 1.96 p_{Eu} Eu_i, if we assume Student's distribution at 95% confidence interval. Here, p_{Re} 0.082 and p_{Eu} 0.164 denotes the relative deviation of the Re and Eu data, calculated in the previous section. Let ε_i denote the distance of the data point from the fitted curve Eu $f(Re)$. *Fig. 4* gives the geometric interpretation; the interval corresponding to 95% confidence is depicted by the dashed ellipse. The way presented here for calculating the parameters is heuristic, it is an arbitrary but straightforward generalization of the least square technique, without inheriting the statistical properties of the least square technique, see [2]. The parameters in (10) are chosen in such a way that the sum of the squared distances ε_i weighted with the inverse of the error bound area $\frac{\pi}{4}\Delta_{Re_i}$ Δ_{Eu_i} should be minimized:

$$\sum_{i\ 1}^{N}\left(\frac{\varepsilon_i}{\frac{\pi}{4}\Delta_{Re_i}\ \Delta_{Eu_i}}\right)^2 \quad \frac{1}{\left(\pi\ 1.96^2\ p_{Re}\ p_{Eu}\right)^2}\sum_{i\ 1}^{N}\frac{\left(Re_i \quad Re_i\right)^2\left(Eu_i \quad Eu_i\right)^2}{Re_i^2\ Eu_i^2} \quad \min, \tag{13}$$

where Re_i and Eu_i are the tangent points on the curve to be fitted. They can be computed by (iteratively) solving the equation

$$Re_i \quad Re_i \quad f\ \left(Re_i\right)\left[Eu_i \quad f\left(Re_i\right)\right]. \tag{14}$$

The result of the curve fitting is given in *Table 2* for several slenderness values.

Table 2. Results for Re_{crit} and Eu_{turb} for several h/D slenderness values, see (10). The disc thickness was h=2 mm for all measurements.

D[mm]	120	224	250	270	285
10^3 h/D	16.7	8.93	7.97	7.41	7.02
Eu_{turb}	2.334	2.265	2.186	2.056	2.041
Re_{crit}	15860	12900	14830	14660	13990

5. Discussion

The main result of the work presented in this paper is that based on experiments, a closed-from analytical relationship was given for computing the breaking torque on a disc rotating in a viscous fluid around its diameter. The relationship is expressed in terms of dimensionless variables, thus – if the geometrical configuration is not changed – it holds for a wide range of disc diameters and angular velocities, both for laminar and turbulent flow conditions. The relationship also provides a smooth

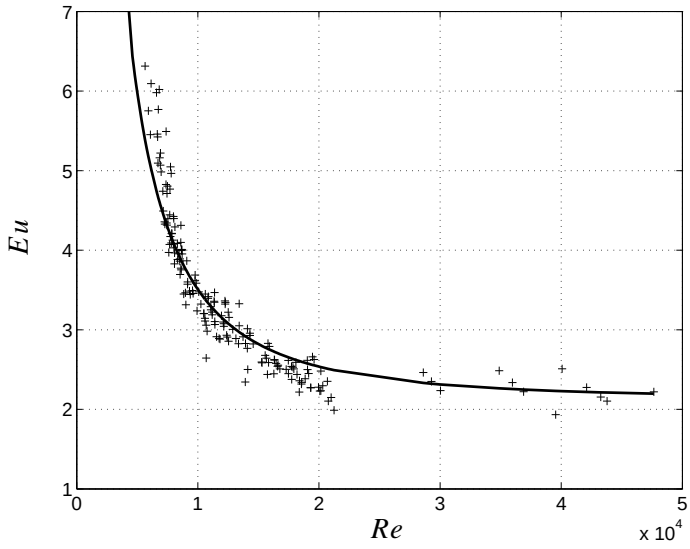

Fig. 5. Measured values and fitted curve for D=285mm.

approximation across the laminar-turbulent transition zone, which is important for analytical calculations.

However, it was clearly shown that the weak point of this measuring technique is the inaccurate measuring of the angular velocity, which introduces a relative error of up to 8%. Thus, one of our future plans is to improve the velocity measurement, e.g. by employing Fourier analysis of the voltage signal of the diode or mounting a water-proof angular velocity measuring instrument. From a more general point of view, it would be interesting to study the effect of wall roughness and also conduct a systematic study in different fluids (notably in air).

References

[1] FONYÓ, ZS. – FÁBRY, GY., *Vegyipari művelettani alapismeretek*. Nemzeti Tankönyvkiadó Rt., Budapest, 1998.
[2] HALÁSZ, G. – HUBA, A., *Műszaki mérések*. Műegyetem Kiadó, 2004.
[3] LAJOS, T., *Az áramlástan alapjai*, Műegyetem Kiadó, 2004.
[4] PANDULA, Z., Merev test szabadesése viszkózus közegben. Master's thesis, Budapest University of Technology and Economics, 1996.
[5] PANDULA, Z., *Dynamic Behaviour of a Check Valve*. PhD thesis, Budapest University of Technology and Economics, Dept. of Hydrodynamic Systems, 2003.
[6] REIMANN, J., *Valószinűségelmélet és matematikai statisztika*. Tankönyvkiadó, 1992.